Science in China Series D: Earth Sciences 2006 Vol.49 Supp. II 24—35

DOI: 10.1007/s11430-006-8024-9

A preliminary study for spatial representiveness of flux observation at ChinaFLUX sites

MI Na[1,2], YU Guirui[2], WANG Panxing[1], WEN Xuefa[2] & SUN Xiaomin[2]

1. Nanjing University of Information Science and Technology, Nanjing 210044, China;
2. Key Laboratory of Ecosystem Network Observation and Modeling, Institute of Geographic Sciences and Natural Resources Research, Chinese Academy of Sciences, Beijing 100101, China

Correspondence should be addressed to Yu Guirui (email: yugr@igsnrr.ac.cn)

Received October 27, 2005; accepted March 10, 2006

Abstract The results of eddy covariance observation system could represent the physical process at certain area of the surface. Thus point-to-area representativeness was of primary interest in flux observation. This research presents a preliminary study for flux observation at ChinaFLUX sites by the use of observation data and Flux Source Area Model (FSAM). Results show that the footprint expands and is further away from flux tower when atmosphere becomes more stable, the observation height increases, or the surfaces become smoother. This suggests that the area represented by the flux observation becomes larger. The distances from the reference point to the maximum point S_{max} and the minimum point x_1 of source weight function (D_{max} and D_{min}, respectively) can be influenced by atmosphere stability which becomes longer when atmosphere is more stable. For more rough surfaces and lower observation point D_{max} and D_{min} become shorter. This research gives the footprint at level P=90% at ChinaFLUX sites at different atmosphere stability. The preliminary results of spatial representiveness at ChinaFLUX sites were given based on the dominant wind direction and footprint response to various factors. The study also provides some theoretical basis for data quality control and evaluating data uncertainty.

Keywords: eddy covariance method, footprint, source weight function, ChinaFLUX.

Eddy covariance method has limited hypothesis in measuring flux in micrometeorology[1], which can be used for long-term measurement of mass and energy exchange between terrestrial ecosystem and atmosphere[2−4]. The instruments for eddy covariance measurement are exposed to different atmospheric conditions and certain height above the physical surface to obtain an estimation of the mass, heat or momentum flux between the (physical) surface and the atmosphere. Thus the results measured by the instruments are supposed to represent processes happening at the surface or a specific portion of the surface[5]. The spatial representativeness of flux observation, i.e. point-to-area representativeness, describes the extent to which the measured results in a point reflect the actual (average or aggregated) conditions over a surface[5]. The relating research could be applied to site selection, observation data quality control and observation up-scaling, etc.[6]. Nappo *et al.*[7] stated that at present there is no quantitative method to determine representativeness. The specific criteria for representativeness based on the acceptable difference between the meas-

ured point value and "true" average flux of the specific surface patch need to be determined. Based on these criteria, the spatial representativeness can be estimated approximately through statistic analysis of the accepted and measured value. Nevertheless, for flux observation, "true" average flux value is difficult to obtain hence difficulty and limitation still exist in the research of spatial representativeness of flux observation. Footprint is defined as the portion of the upstream surface containing the effective sources and sinks contributing to the turbulent exchange processes at a given point in the surface layer or exerting a dominating influence on the properties sampled in an elevated measurement[8,9]. By analysis of footprint, surfaces that have important and unimportant contributions on the measured data can be separated, which contribute to evaluating the influence of surface characteristic on the measured results. In a physical sense, the near limit of the flux footprint is given to be the requirement that emitted trace gas particles have enough time to attain the receptor height and contribute to the flux before being advected downstream. Keeping these limits of the footprint in mind, its extension consequently is highly dependent on the receptor height and the turbulence in which the scalar is dispersed[10,11]. The latter determines turbulent transport, which varies with atmospheric stability regime and surface properties[12]. Therefore, the size and location of footprint instantaneously change with wind direction, measurement height, terrain roughness and boundary layer characteristics, such as the atmospheric stability[5,13−15]. A notion relating footprint is footprint function or called source weight function, which describing the relationship between the spatial distribution of surface sources (or sinks) and a measured signal at certain height in the surface layer. The functional value of the source weight can be interpreted as the relative weight of a given source to contribute to the value at observation point [11]. At present, "footprint" refers to both source area and source weight function. The work on determining the footprint functions is called footprint analysis and the reliable solution of a footprint function would be useful in quality assessment of the measured data to make sure that the fluxes originate from an area that is representative of the areas interested. Footprint analysis is an important tool in evaluating the spatial representativeness of flux observation.

Since the inception of footprint concept in the early 1990s[16,17], experimentalists have embraced enthusiastically devoting to the development of footprint models and their application to field research. For the first time in micrometeorology, determining an area of influence on measurements by physically-based criteria, instead of empirical criteria, became a real possibility. Thus it began to replace the criterion of a 100:1 fetch to height ratio, long held as the golden rule guiding internal boundary layer estimation and a good first guess also for the source area of flux measurements[18]. Analytical footprint models include mathematical simplifications aiming to the theoretical asymptotic of the physical process so as to obtain a simple method to evaluate the spatial representativeness of flux measurements. After about ten years development of analytical footprint models[5, 16, 19−21], SL-model[16], HW-model[19] and FSAM model[5] have been widely used in research work[6,22,23]. Eulerian analytic flux source area model (FSAM), presented by Schmid, which algorithm relies on the inverted plume assumption and the mean wind is parallel but counter to the x-axis direction. Vertical flux divergences are not accounted for, while diffusion in the lateral direction is assumed to be Gaussian. This model has been widely used because of the additional insight provided for experiments over patchy surfaces of modest dimensions. The Lagrangian stochastic approach and large eddy simulation (LES) approach are also methods employed in footprint analysis, in which LES approach holds potential for future studies and is ideally suited to tackle footprint descriptions under inhomogeneous conditions[24].

In China, the eddy covariance technology has been recently applied to large-scale flux measurement of different ecosystems. Establishment of ChinaFLUX has provided a platform for the research of carbon, water and energy exchange between terrestrial ecosystems and atmosphere in China[25]. The analysis of the spatial representativeness of the measurement could provide theory basis for the data quality control and up-scaling of observation. The purpose of this paper is to analyze the influence factors of footprint, discuss the size and location of footprint under differ-

ent environments and evaluate the spatial representativeness of flux measurement by use of observation data and FSAM.

1 Theory and method

1.1 FSAM model

For an observation point at (0, 0, z_m) (Fig. 1),

$$\eta(0,0,z_m) = \int_{-\infty}^{+\infty}\int_{-\infty}^{x} Q_\eta(x,y,z-z_0) \cdot f(-x,-y,z_m-z_0)\cdot dx\cdot dy, \quad (1)$$

x-axis direction is parallel and counter to the wind direction. $f(-x,-y,z_m-z_0)$ relates the value of η at (0, 0, z_m) to the source distribution on the ground and is referred to the source weight function. The value of the source weight function could be interpreted as the relative weight of a given source contributing to the value of δ at the observation point. The value of source weight function is thus dependent on the distance between the source point and the observation point. In an advective situation, most of the passive scalar from sources close-by will not have enough time to be diffused up to z_m before being advected past the reference point. x_1 is the least value of source weight function and the area between reference point and x_1 have little contribution to the measured flux. The value of source weight function is small when separation distance is small. The value of source weight function will rise to a maximum with the increasing distance and then fall off again to all sides as the separation is further increased. The source area of level P was bounded by the isopleth f_P (see near end x_1 and far end x_2 in Fig. 1).

Considering a point source of unit strength at (x_s, y_s, z_0), such that

$$Q_\eta(x,y,z_0) = Q_{\eta,u}\cdot\delta(x_s-x)\cdot\delta(y_s-y), \quad (2)$$

where $Q_{\eta,u}$ is a constant of unit source strength to ensure dimensional consistency and η is the Dirac-delta distribution function. Thus if the convolution of (1) is performed on (2), follows could be obtained:

$$\eta(0,0,z_m) = Q_{\eta,u}\cdot f(-x_s,-y_s,z_m-z_0). \quad (3)$$

Assuming that the concentration distribution of a unit surface point source is of the form[10,26]

$$C(x,y,z) = \frac{D_y(x,y)D_z(x,z)}{U(x)}. \quad (4)$$

Eq. (4) assumes that dispersion in the crosswind direction is independent of height and that dispersion in the vertical direction is independent of crosswind location. $U(x)$ is the effective speed of plume advection in the streamwise direction, x, and is assumed to be independent of y and z. U is constrained

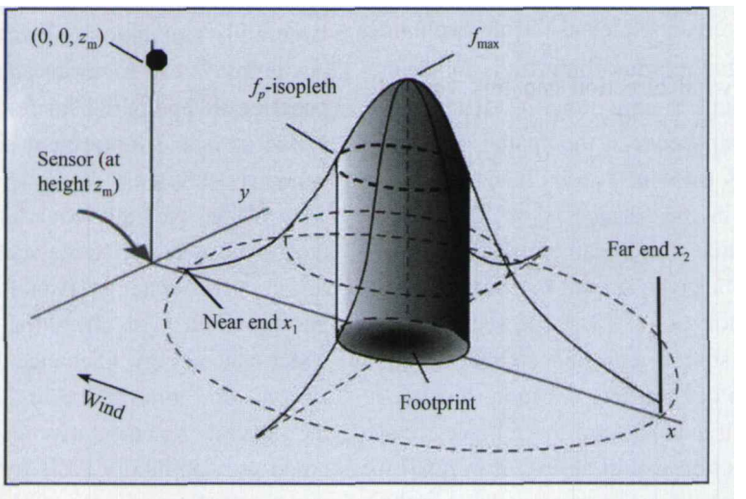

Fig. 1. Footprint and its relation to the footprint function[11].

by mass conservation to be

$$U(x)=\int_0^{\infty} U(z)D_z(x,z)dz, \tag{5}$$

where $U(z)$ is the mean wind speed profile. The crosswind and vertical concentration distribution functions, D_y and D_z, are defined to satisfy the constrains

$$\int_{-\infty}^{+\infty} D_y dy = 1; \quad \int_0^{+\infty} D_z dz = 1. \tag{6}$$

Using K-theory, the vertical eddy flux from a surface source can be represented as a gradient diffusion process

$$f(x,y,z) = -K_c(z)\frac{\partial C(x,y,z)}{\partial z} = -K_c(z)\frac{D_y(x,y)}{U(x)}\frac{\partial D_z(x,z)}{\partial z}, \tag{7}$$

where K_c is eddy diffusivity. Integrating this equation over y, we find the crosswind-integrated footprint to be

$$\overline{f}^y \equiv \int_{-\infty}^{+\infty} f(x,y,z)dy = -\frac{K_c(z)}{U(x)}\frac{\partial D_z(x,z)}{\partial z}. \tag{8}$$

By comparing eqs. (8) and (9), it is apparent that

$$f(x,y,z) = D_y(x,y)\overline{f}^y, \tag{9}$$

i.e., the dependence of the flux footprint on crosswind location is equal to the crosswind concentration distribution from a unit surface point source. In eq. (4), the independence of crosswind and vertical dispersion is assumed. This assumption is likely to be valid in the surface layer. The most likely exception may occur in light-wind, stably-stratified conditions where strong vertical shear of the wind direction can link vertical mixing and horizontal spread of the plume. However, this is unlikely to be significant over the depth of the surface layer. Crosswind dispersion from a point source is observed to produce a concentration distribution that is generally assumed to be Gaussian,

$$D_y(x,y) = \frac{e^{-y^2/2\sigma_y^2}}{\sqrt{2\pi}\sigma_y}, \tag{10}$$

where σ_y is crosswind speed standard deviation, which is commonly expressed as a function of atmospheric stability and distance downwind of the source. The crosswind-integrated footprint is equal to the crosswind-integrated flux downwind of a unit surface point source and thus is related to the crosswind-integrated concentration distribution, $\overline{C^y}$, and mean wind speed profile, $\bar{u}(z)$, through the two-dimensional advection diffusion equation,

$$\bar{u}(z)\cdot\frac{\partial}{\partial x}\overline{C^y} = -\frac{\partial}{\partial z}\overline{f^y}. \tag{11}$$

This equation neglects horizontal turbulent diffusion along the streamlines, in addition to the already mentioned simplifications of height independent crosswind dispersion and first-order closure or gradient diffusion[21]. Integrating eq. (11), the vertical flux at level z_m could be expressed as

$$\overline{f}^y(x,z_m) = -\int_0^{z_m}\bar{u}(z)\cdot\frac{\partial}{\partial x}\overline{C^y}(x,z)\cdot dz. \tag{12}$$

The two-dimensional flux-source weight function becomes

$$f^*(x,y,z) = \frac{F(x,y,z)}{F_u} = \frac{1}{F_u}\overline{F^y}\cdot D_y(x,y), \tag{13}$$

F is vertical turbulent flux, which corresponds to η in eq. (3); F_u is a unit surface point source flux, which corresponds to $Q_{\eta,u}$ in eq. (3)[5,19].

1.2 Running FSAM

Input parameters for FSAM running include friction velocity, Obukov length, crosswind speed standard deviation, roughness length, measurement height, zero-plane displacement. The results of the model are presented as the location of maximum source point, characteristic dimensions of source area and the location of minimum point of source weight function at level P=10%−90%. Detail introduction to the input and output parameters of model can be referred to Zhao[27]. Difference from Zhao in this paper is that z_0 is prescribed as an empiristic value for each site during growing season (see Table 1). In addition, FSAM has its restriction on z_m/z_0, z_m/L and σ_v/u_*[11],

under stable conditions:

$2.0\cdot10^1 \leqslant z_m/z_0 \leqslant 5.0\cdot10^2$,

$2.0\cdot10^{-4} \leqslant z_m/L \leqslant 1.0\cdot10^{-1}$,

$1.0 \leqslant \sigma_v/u_* \leqslant 6.0$;

under unstable conditions:

$$4.0\cdot10^{1} \leqslant z_m / z_0 \leqslant 1.0\cdot10^{3},$$

$$4.0\cdot10^{-4} \leqslant -z_m / L \leqslant 1.0,$$

$$1.0 \leqslant \sigma_v / u_* \leqslant 6.0.$$

2 Description of sites and dataset selection

2.1 Description of sites

At present, ChinaFLUX consists of 8 sites, which include four forest sites (Changbaishan, Qianyanzhou, Dinghushan, and Xishuangbanna), three grassland sites (Haibei, Inner Mongolia, and Dangxiong) and a cropland site (Yucheng). These sites cover the main ecosystem types in China. The brief descriptions of sites are listed in Table 1.

2.2 Dataset processing

Flux data and routine meteorological data of one year for 8 sites in ChinaFLUX are selected for investigation. Measuring period at DX site only covered eight months because it was established in the year 2003. Potential temperature (θ_v), friction velocity and $\overline{W'\theta_v'}$ are used to calculate atmospheric stability. Meteorology data are used in wind direction statistics. In order to eliminate the items of horizontal and vertical advection in the equation of conservation of mass, the 30 min flux data are reformed by three-dimension coordinate rotation. After the above corrections, the irrational data such as observations during precipitation events were deleted. The final dataset consists of 15872, 6491, 13998, 12793, 13290, 14259, 15083, 26679[1)] records in YC, DX, HB, NMG, QYZ, XSBN, DHS and CBS.

3 Results

3.1 Factors effect on footprint

(i) Influences of wind direction. Footprint of flux observation distributed in upwind area. In order to discuss the distribution of flux footprint, it is necessary to make statistics of wind direction of each site. Statistics of wind direction for each site is illustrated in Fig. 2.

From Fig. 2 we can see that the occurrence frequency of wind direction at ChinaFLUX site shows "two peaks" except at DX and CBS sites, which means that there are two prevail wind directions for a year due to monsoon climate in China. Prevail wind direction at each site is northeastern and south at YC and HB sites, northwest and south at NMG site, northwest and southeast at QYZ site, west and east at XSBN site, northeast and southwest at DHS site; southwest at CBS site.

(ii) Influences of measurement height. Taking QYZ site for an example, two open path eddy covariance systems were installed on double- (23.6 m) and triple-height (39.6 m) of vegetation, respectively. Fig. 3 gives the size and shape of footprint and maximum source point at level P=90% on two measurement heights.

Fig. 3 shows that footprint increases and moves

Table 1 Summary of the ChinaFLUX sites in this study

Site	Lon.(°E)	Lat.(°N)	Vegetation [a)]	z_m(m)	z_0[b)](m)	d[c)](m)	Vegetation height (m)	IRGA[d)]	Time range
CBS	128.10	42.40	DBCMF	41.5	1.0	17.3	26	O/C	02-9-1 — 03-8-31
QYZ	115.07	26.73	MPF	23/39	0.5	8	12	O/C	03-1-1 — 03-12-31
DHS	112.53	23.17	EBF	27	0.6	10	15	O	03-1-1 — 03-12-31
XSBN	101.20	21.95	TSRF	48.8	1.2	23.3	35	O	03-1-1 — 03-12-31
NMG	117.45	43.50	grassland	2.2	0.03	—	0.45	O	03-5-16 — 04-5-15
HB	101.30	37.60	alpine meadow	2.2	0.03	—	0.5	O	03-1-1 — 03-12-31
DX	91.08	30.85	alpine meadow	2.2	0.01	—	0.1-0.2	O	03-7-19 — 04-3-18
YC	116.60	36.95	cropland	2.2	0.05	—	1	O	03-1-1 — 03-12-31

a) DBCMF: Deciduous broad-leaved and coniferous mixed forest; MPF: man-planted forest; EBF: evergreen broad-leaved forest; TSRF: tropical seasonal rainforest. b) z_0 is empiristic value. c) Using d = 2H/3 for calculating zero-plane displacement, H is average vegetation height. For grassland and cropland, d is neglected. d) O: Open path system; O/C: open/close path system.

1) 2002-9-1—2003-3-27 at CBS site, 15 min were adopted as averaging period

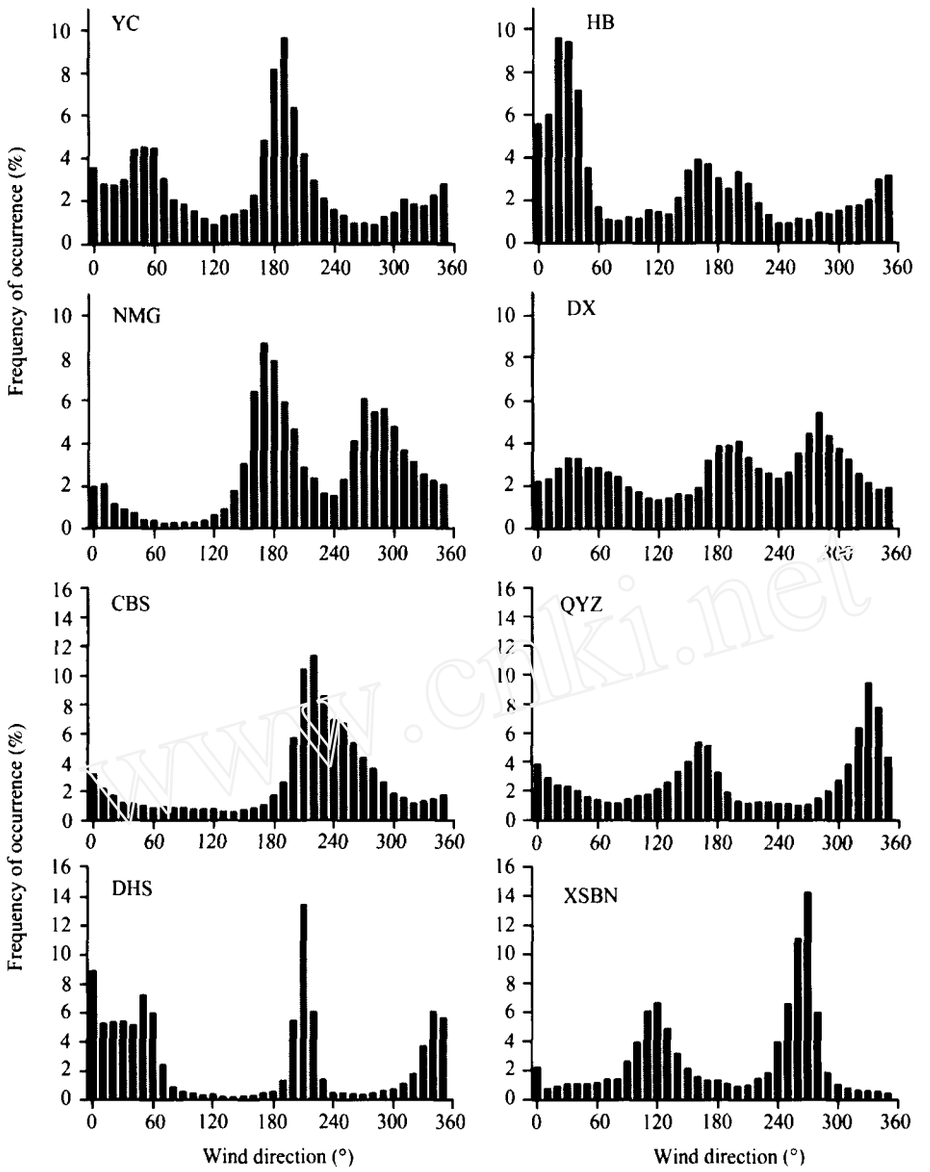

Fig. 2. Wind direction and its occurrence frequency at ChinaFLUX sites.

further away from flux tower with the increase of observation height. For the eddy covariance system installed at 39.6 m, the calculated footprint has a length of 1915 m. In contract, the footprint for the eddy covariance system installed at 23.6 m decreased to 1 km. The distance from flux tower to the maximum source point for 23.6 and 39.6 m measurement heights is 248 and 525 m, respectively. The distance from flux tower to x_1 is 102 and 228 m, respectively. Thus source area becomes larger and distances from flux tower to maximum source point and minimum point of source weight function become longer when observation height becomes higher.

(iii) Influences of terrain surface roughness. Cropland flux site was set up in Yucheng, Shandong Province. Terrain roughness varies from season to season due to the fact that crop growing causes changes of vegetation height. This research takes winter wheat in Yucheng for an example to discuss the influence of terrain roughness on footprint size. The height of winter wheat and its corresponding z_0 in 2003 is listed in Table 2.

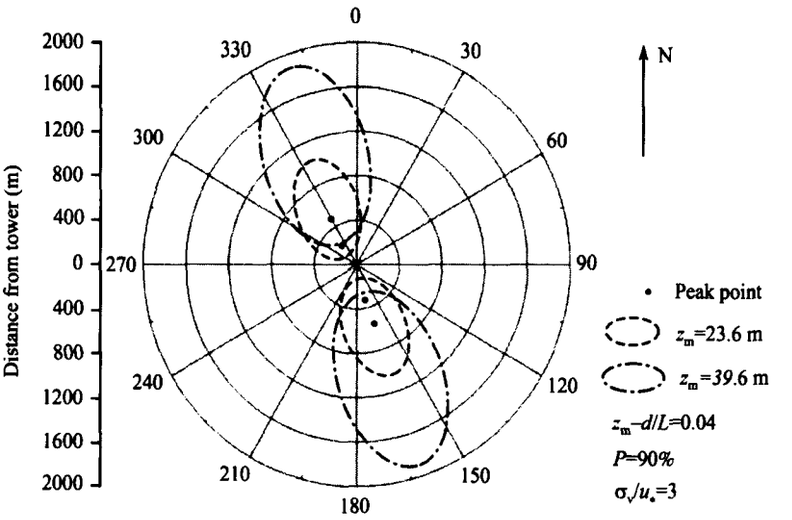

QYZ

Fig. 3. Effects of receptor height on footprint. Center of disc is the location of flux tower. z_m/L and σ_v/u_* are average values for a year after filtering invalid value. Dashed and dot-dashed lines are domain of footprint for the two measurement heights, respectively. The location of footprint is on the direction of prevail wind.

Table 2 The height of winter wheat and its corresponding z_0 in Yucheng

Date	Mar. 20	Mar. 25	Mar. 31	Apr. 8	Apr. 16	Apr. 30	May 7
Vegetation height (m)	0.18	0.25	0.30	0.41	0.62	0.74	0.81
z_0 [a)] (m)	0.0028	0.0056	0.0118	0.0256	0.0377	0.0296	0.0298

a) The method used for calculating z_0 refers to Zhou[28].

Fig. 4 shows that the distance from reference point to x_2 increases from 106 to 122 m, with the decreases of terrain roughness, but it is still within the fetch. Footprint moves further away from flux

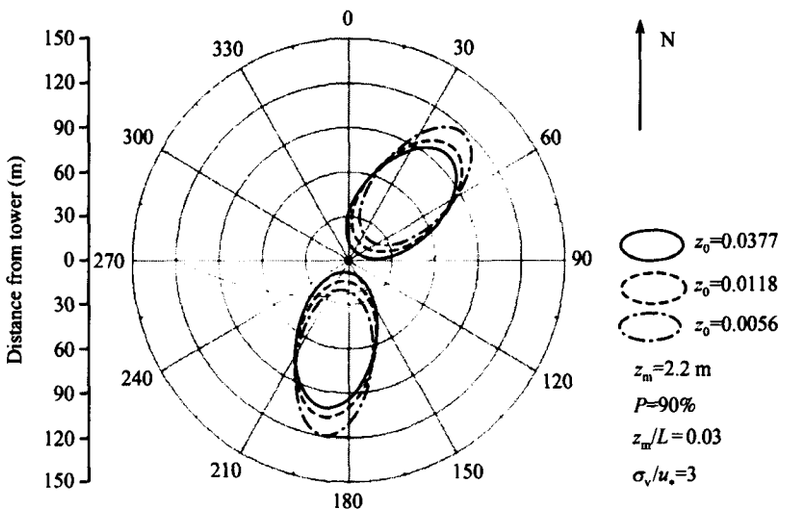

YC

Fig. 4. Effects of terrain roughness on footprint. Center of disc is the location of flux tower. z_m/L and σ_v/u_* are average values for growing season after filtering invalid value. Solid, dashed and dot-dashed lines are domain of footprint for different terrain roughness, respectively. The location of footprint is in the direction of prevail wind.

tower and the distance from observation point to maximum source point increases from 27 to 34 and 39 m. Ranges from flux tower to x_1 for three different growing stages are 11, 15 and 18 m, i.e. the minimum source point is away from observation point versus decreasing of roughness length.

(iv) Influences of atmospheric stability. In boundary layer meteorology, $\zeta = z/L$ is used to represent stability, where L is Obukhov length, z is reference height (= effective height $z_m - d$ in this research). The sign of ζ relates to the stability of atmosphere: Positive means stable while negative means unstable[27]. The size and shape of footprint change with atmospheric stability instantaneously. In this research, taking QYZ and DHS sites for an example, the increase of footprint for three extreme conditions (ζ= −1.0, 0, 0.1) is shown in Fig. 5(a) and (b).

Fig. 5 shows that two edges of footprint at DHS site under unstable atmospheric conditions departs from flux tower 17 and 129 m, which is 94 and 954 m for neutral conditions and 137 and 1908 m for stable conditions. At CBS site, the corresponding distances are 23 and 181 m, 130 and 1430 m, and 190 and 3070 m. It can be seen that footprints become larger and further away from reference point with increasing stability. At the same time, the distances from maximum source

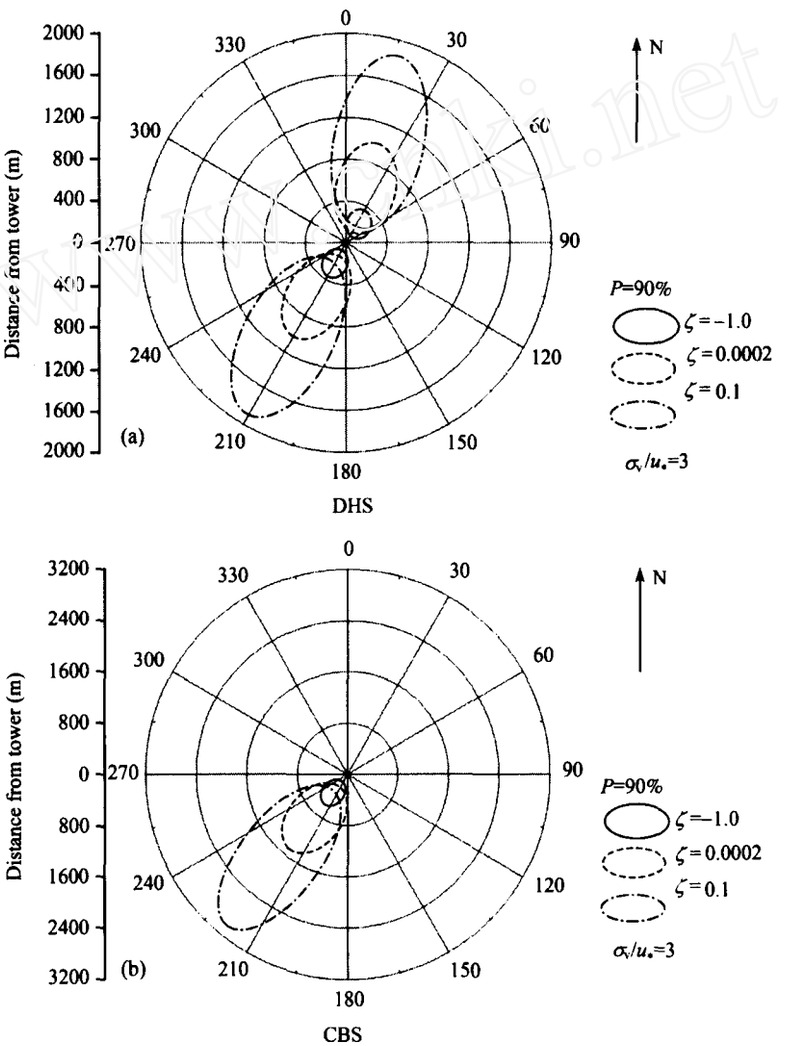

Fig. 5. Effects of atmospheric stability on footprints. Using ζ = −1.0, 0.0002, 0.1 to represent atmospheric stability, neutral and instability conditions, respectively. Solid, dashed and dot-dashed lines are domain of footprint for different atmospheric stability, respectively. The location of footprint is on the direction of prevail wind.

point and minimum source point to flux tower become longer. The pattern can be contributed to the following reasons. Strenuous vertical kinetic and quickly vertical transport under unstable atmospheric conditions make the measured flux originating from nearer surface and the source area is relatively small. While under stable atmosphere, turbulence is weak with slower vertical material transport which makes the observed flux originating from further surface and the source area is relatively large[27].

3.2 Maximum source point location

When source weight function reaches its maximum (f_{max}), the projection of f_{max} on the land surface is maximum source location (S_{max}). Distance (D_{max}) from flux tower to maximum source point for each flux site of ChinaFLUX is calculated using FSAM. The location of f_{max} is different under different atmospheric conditions. Table 3 gives the range of D_{max} at each of the ChinaFLUX site.

3.3 Minimum point of source weight function

The projection of minimum point of source weight function on the land surface is the near end (x_1) and the area from flux tower to x_1 has little contribution to the measured flux. The distances from flux tower to x_1 for each flux site of ChinaFLUX are presented in Table 4. Similar to the maximum source point, the distances from x_1 to flux tower also changed with atmospheric conditions.

3.4 Footprint prediction

The size and shape of footprint changed with atmospheric conditions under a given roughness length and measurement height. Table 5 gives the length of footprint for each site of ChinaFLUX under various atmospheric conditions.

The distribution of footprint for each site can be approximately estimated from the results shown in Tables 4, 5 and section 3.1. For example, under unstable atmospheric conditions ($\zeta = -1.0$), footprint at NMG site distributed in the surrounding area of the flux tower ranged from 3 to 19 m and it is mainly on Northwest and South which is the direction of prevail wind. Under near neutral conditions, footprint moves further away from flux tower and its area becomes larger, which ranged from 14 to 110 m. When atmosphere become more stable ($\zeta = 0.1$), footprint distributed in the surrounding area of the flux tower ranged from 19 to 195 m.

4 Discussion

4.1 Application of FSAM

The FSAM is based on physical method and can be easily used for the calculation of areas that contribute to the measured fluxes. However, FSAM has the disadvantage of being applied only under near neutral condition and requiring horizontal homogeneity. This algorithm is based on the analytic footprint model by

Table 3 Distance from flux tower to maximum source point for each flux site of ChinaFLUX[a)]

Site	YC	HB	NMG	DX	QYZ	DHS	CBS	XSBN
D_{max} (m)	5−43	7−48	7−48	10−50	29−335	29−365	38−521	38−550

a) The values in Table 3 represent the results of ζ=1.0, 0.1. The results for QYZ is measured on z_m=23.6 m.

Table 4 Distance from minimum point of source weight function to flux tower for each flux site of ChinaFLUX/m[a)]

Sites		YC	HB	NMG	DX	QYZ	DHS	CBS	XSBN
Atmosphere stability	instability	2	3	3	5	16	17	23	24
	neutral	12	14	14	16	88	94	130	133
	stability	17	19	19	22	128	137	190	212

a) The values in Table 4 represent the results of $\zeta = -1.0$, 0.0002, 0.1. The results for QYZ is measured on z_m=23.6 m.

Table 5 The length of footprint for each site of ChinaFLUX/m[a)]

Sites		YC	HB	NMG	DX	QYZ	DHS	CBS	XSBN
Atmosphere stability	instability	16	19	19	27	120	129	181	188
	neutral	104	110	110	111	855	954	1430	1584
	stability	190	195	195	163	1655	1908	3070	2808

a) The values in Table 5 represent the results of $\zeta = -1.0$, 0.0002, 0.1. The results for QYZ is measured on z_m=23.6 m. P=90%

Horst and Weil[10], and employs an extended version of the surface-layer dispersion model by Gryning *et al.*[30] For the determination of the crosswind and vertical concentration distribution functions, FSAM assumes a constant flux layer with sources located only at the ground. The model is restricted to scale of near surface layer and air flow has to be horizontally homogeneous. The performance of the FSAM- algorithms is very sensitive to the input of the roughness length, because the input parameters of roughness length, measurement height, and Obukhov length are internally normalized by z_0. The FSAM is only applicable to a certain range of conditions, as specified by the ratios of measurement height and roughness length, measurement height and Obukhov length, and standard deviation of crosswind velocity and friction velocity (see section 1.2).

Lagrangian stochastic footprint model is a method superior to analytical model because it considers transport processes within the canopy space as well as alongwind diffusion[31]. Its modeling results have been tested with observation data[32]. Comparison has been made between modeling results of FSAM and Lagrangian stochastic model and the result suggests that the analytic FSAM model overestimates the source areas[6]. If this is proved by further studies, the site evaluation approach could be further improved by the integration of the Lagrangian stochastic footprint model. This research tries to make analysis of spatial representativeness using a simple method. Stochastic models are not used in this study because they need several additional parameters to be fitted to specific site conditions, which is difficult for practical applications.

4.2 The limitation of surface conditions

FSAM assumes that the surface is simple and has no disturbance by obstacle building and terrain. It can be applied in a forest and assumes that the (closed) canopy top is the surface. Most of forest sites of ChinaFLUX are located in complex terrain that cannot fully satisfy the requirement of FSAM hypothesis. Hence, the results of this research may have errors and they can only be used for reference in the actual work. Further development of model suitable for complex terrain applications is required. Although some progress has been made it is still a hotspot research area in flux measurement studies[33].

4.3 The application of flux observation spatial representativeness

The results of this research show that with the increase of measurement height, atmospheric stability, and the decrease of roughness length, the footprint area increases. The result was consistent with Schuepp's findings[14]. Under stable conditions, footprints of high vegetation in the complex terrain often exceed the field that researchers interested, which lead to the uncertainty of measurement results. Further quantitative research on footprint can provide theoretical basis for data quality control and assurance of observation data validity.

Eddy covariance technique requires that the surface of observation site is flat, homogeneous and has enough fetch. If the above conditions can be satisfied, the selection of location for flux tower should not be a problem. But in reality many sites are set up among the tall forest with heterogeneous surface. This brings uncertainties to flux observation data. Footprint analysis through determining the distribution of footprint applies its results into flux tower site selection, observation data quality evaluation and control. Göckede[6] applied FSAM to complex terrain through alterative method and results show that this model can provide considerable estimation as a tool of data quality evaluation[34]. Results of this research on the evaluation of spatial representativeness of ChinaFLUX are given in Table 6.

Fetch of each flux site satisfies the footprint requirement considerably. The result of CBS is smaller than the estimation of Zhao[27] which attributes to the different values of roughness length. In addition, there is a lake within the footprint at DHS site, which should be considered when analyzing vapor flux.

5 Conclusions

Preliminary study for the spatial representativeness of ChinaFLUX observation sites has been made using FSAM and observation data. The impact factors that affect footprints are analyzed. The changing pattern of the maximum source point and the minimum point of

Table 6 Source of information of each flux site and its proportion

Sites	Source of information	Proportion (%)	The smallest extention of footprint (m)	The largest extention of footprint (m)
CBS	Broad-leaf Korean pine forest from northwest to north east	74	181	3070
QYZ	Man-planted forest distributed in northwest and southeast (*Pinus massoniana, Pinus elliottii Engelm, Cunninghamia lanceolata*)	74	120	1655
DHS	Southern subtropical evergreen mixed forest distributed in northeast and southwest (*Castanopsis chinensis, Schima superba, Pinus massoniana*)	81	129	1908
XSBN	Tropical seasonal rainforest distributed in the west and east (*Castanopsis hystrix, Castanopsos Indica*)	72	188	2808
NMG	Guinea grass distributed in west and south	74	19	195
HB	Alpine meadow distributed in northeast and south	70	19	195
DX	Alpine meadow distributed in northeast, south and west	78	27	163
YC	Wheat-Zea mais distributed in northeast and south (crop rotation)	71	16	190

source weight function also has been investigated. Finally, the spatial representativeness for ChinaFLUX is evaluated by combining the above results.

(1) In general, footprint expands and moves further away from flux tower when atmosphere becomes more stable, observation height is higher, and surface becomes smoother, which suggests the area contributing to the measured flux becomes larger. At the same time, distances from reference point to maximum source point and minimum point of source weight function become longer.

(2) The length of footprint for each site of ChinaFLUX at level 90% is presented in this research. Preliminary results for the spatial representativeness at each site is given based on the local prevail wind direction and influencing patterns of environmental factors. Results show that the fetch of each site of ChinaFLUX could satisfy the request of footprint and more than 70 percent fluxes of each site come from the ecosystem that researchers focused on.

(3) Research on methodology of flux observation on complex terrain is a hotspot in international fluxes studies. Although this research is only regarded as a reference in actual work, it could provide some theoretical basis for data quality assessment and control, observation up-scaling and evaluating data uncertainties.

Acknowledgements The authors are much grateful to Dr. Shusen Wang for his help in preparation of the manuscript. This work was supported by the Knowledge Innovation Program of the Chinese Academy of Sciences (CAS) "Study on Carbon Budget in Terrestrial and Marginal Sea Ecosystems of China" (Grant No. KZCM1-SW-01), and the National Key Basic Research and Development Program of the Ministry of Science and Technology of the People's Republic of China "Carbon Cycle and Driving Mechanism in Chinese Terrestrial Ecosystem (Grant No. 2002CB412500).

References

1 Foken T, Wichura B. Tools for quality assessment of surface-based flux measurements. Agri Forest Meteorol, 1996, 78: 83—105
2 Aubinet M, Grelle A, Ibrom A, et al. Estimates of the annual net carbon and water exchange of European forests: the EUROFLUX methodology. Adv Ecol Res, 2000, 30: 113—175
3 Baldocchi D, Finnigan J, Wilson K T, et al. On measuring net ecosystem carbon exchange over tall vegetation on complex terrain. Boundary-Layer Meteorol, 2000, 96: 257—291
4 Baldocchi D. Assessing the eddy covariance technique for evaluating carbon dioxide exchange rates of ecosystems: past, present and future. Global Change Biology, 2003, 9: 479—492
5 Schmid H P. Experimental design for flux measurements: matching the scales of observations and fluxes. Agri and Forest Meteorol, 1997, 87: 179—200
6 Göckede M, Corinna R, Foken T. A combination of quality assessment tools for eddy covariance measurements with footprint medelling for the characterization of complex sites. Agri Forest Meteorol, 2004,127: 175—188
7 Nappo C J. The workshop on the representativeness of meteorological observation. June 1981, Boulder, CO. Bulletin of America Meteorology Society, 1982, 63: 761—764
8 Schmid H P, Oke T R. A model to estimate the source area contributing to turbulent exchange in the surface-layer over patchy terrain. Quar J Royal Meteorol Soc, 1990, 116: 965—998
9 Wilson J D, Swaters G E. The source area influencing a meas-

urement in the planetary boundary-layer: the footprint and the distribution of contact distance. Boundary-layer Meteorol, 1991, 55: 25－46

10 Horst T W, Weil J C. Footprint estimation for scalar flux measurements in the atmospheric surface-layer. Boundary-Layer Meteorol, 1992, 59: 279－296.

11 Schmid H P. Source areas for scalars and scalar fluxes. Boundary-Layer Meteorol, 1994, 67: 293－318

12 Kljun N, Kastner-Klein P, Fedorovich E, et al. Evaluation of a Lagrangian footprint model for a wide range of boundary layer stratification. Agri Forest Meteorol, 2004, 127: 189－201

13 Rannik Ü, Aubinet M, Kurbanmuradov O, et al. Footprint analysis for measurements over a heterogeneous forest. Boundary-Layer Meteorol, 2000, 97: 137－166

14 Kljun N, Rotach M W, Schmid H P. A 3-D backward Lagrangian footprint model for a wide range of boundary layer stratifications. Boundary-Layer Meteorol, 2002, 103: 205－226

15 Schmid H P. Footprint modeling for vegetation atmosphere exchange studies: a review and perspective. Agri Forest Meteorol, 2002, 113: 159－283

16 Schuepp P H, Leclerc M Y, Macpherson J I, et al. Footprint prediction of scalar fluxes from analytical solutions of the diffusion equation. Boundary-Layer Meteorol, 1990, 50: 353－373

17 Leclerc M Y, Thurtell G W. Footprint prediction of scalar fluxes using a Markovia analysis. Boundary-Layer Meteorol, 1990, 52: 247－258

18 Vesala T, Rannik Ü, Leclerc M. Flux and concentration footprints. Agri Forest Meteorol, 2004, 127: 111－116

19 Horst T W, Weil J C. How far is far enough-the fetch requirements for micrometeorological measurement of surface fluxes. J Atmos Ocean Tech, 1994, 11: 1018－1025

20 Haenel H D, Grünhage L. Footprint analysis: a closed analytical solution based on height-dependent profiles of wind speed and eddy viscosity. Boundary-Layer Meteorol, 1999, 93: 395－409

21 Kormann R, Meixner F X. An analytic footprint model for neutral stratification. Boundary-Layer Meteorol, 2001, 99: 207—224

22 Kutsch W L, Liu C H, Hörmann G, et al. Spatial heterogeneity of ecosystem carbon fluxes in a broadleaved forest in Northern Germany. Global Change Biol, 2005, 11: 70－88

23 Hollinger D Y, Aber J, Dail B, et al. Spatial and temporal variability in forest-atmosphere CO_2 exchange. Global Change Biol, 2004, 10: 1689－1706

24 Leclerc M Y, Shen S H, Lamb B. Observation and large-eddy simulation modeling of footprints in the lower convective boundary layer. J Geophy Res-Atm, 1997, 102: 9323－9334

25 Yu G R, Zhang L M, Sun X M, et al. Advances in carbon flux observation and research in Asia. Sci China Ser D-Earth Sci, 2005, 48 (Supp. I): 1－16

26 Pasquill F, Smith F B. Atmospheric Diffusion. 3rd ed. New York: Wiley, 1983. 437

27 Zhao X S, Guan D X, Wu J B, et al. Distribution of footprint and flux source area of the mixed forest of broad-leaved and Korean pine in Changbai Mountain. Journal of Beijing Forest University (in Chinese), 2005, 27(3): 17－23

28 Zhou Y L, Sun X M, Zhu Z L, et al. Surface roughness length dynamic over several different surfaces and its effects on modeling fluxes. Sci China Ser D-Earth Sci, 2006, 49(Supp.II): 262－272

29 Stull R B. An introduction to boundary layer meteorology. Kluwer: Academic Press, 1988

30 Gryning S E, Holtslag A A M, Irwin J S, et al. Applied dispersion modeling based on meteorological scaling parameters. Atm Environ, 1987, 21: 79－89

31 Baldcchi D. Flux footprints within and over forest canopies. Boundary-Layer Meteorol, 1997, 85: 273－292

32 Finn D, Lamb B, Leclerc M Y, et al. Experimental evaluation of analytical and Lagrangian surface-layer footprint model. Boundary-Layer Meteorol, 1996, 80: 283－308

33 Sogachev A Y, Rannik Ü, Vesala T. Flux footprints over complex terrain covered by heterogeneous forest. Agri Forest Meteorol, 2004, 127: 143－158

34 Rebmann C, Göckede M, Foken T, et al. Quality analysis applied on eddy covariance measurements at complex forest sites using footprint modeling. Theor App Climatol, 2005, 80: 121－141